39th AIAA Fluid Dynamics Conference
22 - 25 June 2009, San Antonio, Texas

AIAA 2009-3566

Perturbation of a turbulent boundary layer by spatially-impulsive dynamic roughness

B J. McKeon, I. Jacobi & J. LeHew*

First experimental measurements of manipulation of the structure of a canonical zero pressure gradient turbulent boundary layer using a low frequency (compared to the viscous frequency) mechanical dynamic roughness are presented. "Dynamic" (or time-dependent) surface roughness is proposed as a method for both control and diagnosis of turbulent boundary layers.

I. Introduction

The ubiquity of wall-bounded flows in nature and industry make the potential impact of artificial manipulation as enticing as the academic challenges that it presents. It is clear that large gains in terms of both understanding of fluid physics and vehicular efficiency are theoretically possible, at least in flows where large amplification of input disturbances is possible. Equally it is assumed that active flow control, in which actuation is optimized to achieve a particular objective given local time-dependent flow conditions, will be used to reduce the environmental impact of the human transportation explosion, although few active schemes appear to be close to production.

Much previous work on the active control of turbulent wall-bounded flows has focused on the interaction of the flow with discrete actuators, requiring complex modeling. In this paper we focus on the use of a "morphing surface" to manipulate, interrogate and ultimately control wall-bounded flows, where the actuation corresponds to local or global changes to the surface morphology. Active optimization of surface morphology is at present almost exclusively confined to the biological world. The cuttlefish is perhaps unique in the aquatic kingdom in its ability to *actively* change the surface morphology (and color) of its skin by activating chromatophores, leucophores and iridophores (three-color dye sacs) for almost instantaneous concealment.

We seek to isolate this mechanism as an actuation input to manipulate a turbulent boundary layer, introducing for the first time a roughness timescale alongside the distribution of roughness lengthscales associated with rough surfaces and expanding on current understanding of static roughness effects. The introduction of a roughness timescale via a time-varying roughness amplitude can alternatively be viewed as a structured energy addition at the wall. The influence of roughness, and specifically the imposition of new lengthscale(s), on boundary layer flow is a topic of fundamental importance for the understanding and prediction of turbulence structure. It also has important implications for control of skin friction and associated improvements in vehicular efficiency. As such, canonical rough-wall turbulent flows have received a resurgence of interest in recent years, e.g. Jimenez (2004), Flack *et al.* (2005), Gioia & Chakraborty (2006) and Allen *et al.* (2007).[1234]

The influence of a spatially-distributed roughness with a time-varying amplitude has not been so extensively explored. Much previous work on the active control of turbulent wall-bounded flows has focused on the interaction of the flow with discrete actuators, ranging from a single bump rising into a channel flow (Carlson & Lumley 1996)[5] and "active" dimples (McKeon *et al.* 2004),[6] to time-dependent wall motion (Endo & Kasagi 2001; Kim *et al.* 2003)[7,8] However in laminar and transitional flows White & Saric (2000)[9] investigated the use of pneumatically-controlled leading-edge roughness elements to suppress secondary cross-flow instabilities and Honsaker & Huebsch (2005)[10] performed a computational study of variable roughness for the control of laminar boundary layer separation from an airfoil. In this paper we investigate the influence of "dynamic" roughness (where the term "dynamic" implies a time-dependent amplitude imposed on a distributed array of geometric perturbations to an otherwise smooth wall) on a zero pressure gradient turbulent boundary layer.

An ongoing experimental program at Caltech seeks to investigate several aspects of "dynamic" roughness in order to diagnose and manipulate the structure of turbulent boundary layers. A further extension of this work is the use of this technique as an actuation input for low effort manipulation and/or control of a receptive flow, i.e engaging the

*Graduate Aerospace Laboratories, California Institute of Technology, Pasadena, USA

non-linear nature of the turbulent boundary layer to amplify actuation input. This method of actuation has the potential to be used either in an on-demand, "on/off" configuration to selectively change local skin friction or, potentially, with time-dependent motion in order to maintain a particular (to be determined) optimized boundary layer state (with a long-range goal of skin friction reduction). The current work also seeks to enhance our understanding of turbulent boundary layer structure in order to address this latter application.

The resolution requirements imposed by the need to fully-resolve the smallest scales in the turbulent boundary layer at high Reynolds numbers and the geometry associated with a dynamically rough wall suggest that this problem is best addressed experimentally, at least at present. Experimental approaches can afford large enough Reynolds numbers for the separation of the characteristic roughness length, denoted here by k, viscous and outer scales, i.e. conditions such that both $k/\delta \ll 1$ and $k^+ = ku_\tau/\nu \gg 1$, leading to the potential for a fully-rough, high Reynolds number flow in the presence of widely-distributed roughness. Here the friction velocity $u_\tau = \sqrt{\tau_w/\rho}$ is defined in terms of the wall shear stress τ_w and the fluid density ρ, and ν is the kinematic viscosity. However the information that can be obtained by interrogation of the flow is essentially (currently) limited to point or planar measurements.

Previous computational investigations of wall turbulence incorporating models for flow over (statically) rough walls include an examination of the linearized, time-independent problem using wall velocity perturbations by Orlandi (2003)*et al*[11] (where an instantaneous velocity distribution in a plane separating a roughness cavity and the outer flow in a full rough-wall DNS was imposed as the wall boundary condition) and the study of Flores & Jimenez (2006)[12] (in which wall velocities with moments similar to those observed over rough walls were prescribed). Jimenez *et al* (2001)[13] have also modeled flow over active and passive porous walls using wall velocity disturbances.

In this study, interrogation of the turbulent boundary layer as a black box was performed by imposing a perturbation to the wall boundary condition that is sudden spatially, and studying the response and subsequent relaxation of the boundary layer towards equilibrium. Both static (time-independent) and dynamic roughness strip elements, designed to approximate a spatial impulse by imposing step changes of wall boundary condition from smooth-to-rough and rough-to-smooth over a length that is small with respect to the boundary layer thickness are considered. The amplitude of the perturbation is limited by the need to preserve the boundary layer approximation, but both self-similar and severe changes to the turbulence structure are ultimately of interest.

Step changes in roughness beneath a self-similar turbulent boundary layer have been investigated in the context of the response of the layer to a sudden, localized perturbation that may be sufficiently large to disrupt local self-similarity but not so severe that the boundary layer approximations are violated[14151617]. For sufficiently small disturbances, the boundary layer can be considered to be at least approximately self-preserving. However, for more severe spatial step changes in roughness condition[1415] the initial disturbance is confined to the wall region, propagating outwards through an internal layer of thickness $\delta_i(x)$ before undergoing the structural changes required for a return to a self-similar structure at some distance downstream. Approximately impulsive disturbances, as depicted in figure I, introduce two internal layers and have been shown to lead to significantly more complex flow physics than would be indicated by considering two closely consecutive step changes[17] (as consideration of the nonlinear nature of the boundary layer would suggest).

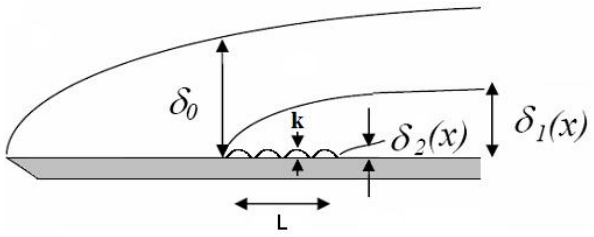

Figure 1. Schematic of the development of internal layers associated with an approximation to a spatial roughness impulse.

II. Experimental Method

Experiments were performed in the $2' \times 2'$ wind tunnel at Caltech in a zero pressure gradient (ZPG) turbulent boundary layer. The test section of the tunnel had an rms variation in pressure of $1.7 - 1.9$ Pa over a length of 1.15 m, or a variation in pressure coefficient, $\Delta C_p \ll 0.01$. A spatial impulse disturbance of two-dimensional, k-type[18] roughness was introduced at a streamwise position corresponding to a local Reynolds number based on momentum

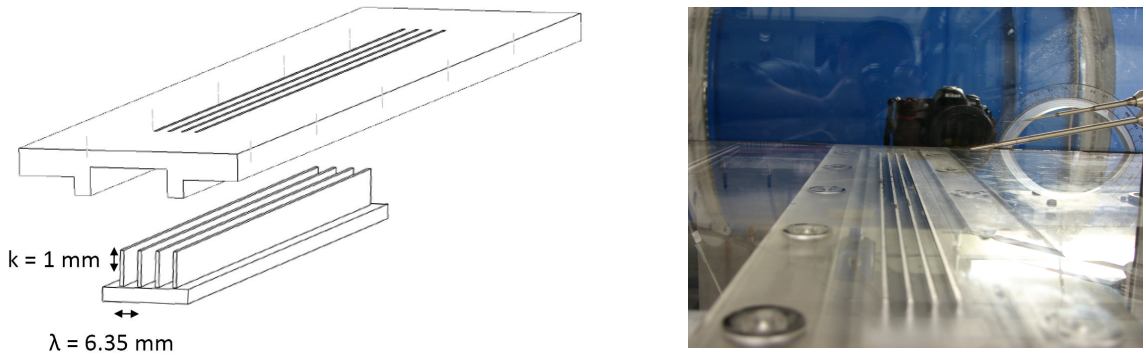

Figure 2. Dynamic roughness apparatus.

thickness, $Re_\theta = 2600$ (figure 2). The time-periodic roughness amplitude was generated using a two-dimensional roughness pattern which fit into channels carved into the test plate such that the roughness elements could move freely through the plate. The four channels were separated by 6.35 mm and were filed to provide a precise fit for the 1.57 mm thick roughness elements; the total roughness area begins 880 mm from the leading edge and extends for 25.3 mm in the streamwise direction, approximately one and a half boundary layer thicknesses. The roughness was driven by a 480 mm narrow piston which connected to a reciprocating motor positioned beneath test section of the wind tunnel. The crankshaft was machined with a 1 mm crank radius and 30 mm rod length, to achieve an order 1 mm amplitude motion. The crankshaft was affixed to a $1/35$ HP, 1800 RPM A/C motor to produce a 30 Hz cycle for the roughness elements.This repeatable mechanical arrangement can easily be modifed via the crank radius or choice of motor to achieve a variety of different roughness amplitudes and frequencies.

Both static and time-varying roughness elements were considered. The peak amplitude achieved by the roughness was 909 ± 45 microns or about 0.9 mm, and $k/\delta = 0.054$; for the dynamic case $f\delta/U_\infty = 0.0249$. The friction between the moving roughness elements and the plate induced a small amplitude, local vibration into the plate of order 10 microns, at the driving frequency, which thus corresponded to a velocity signal $\ll 1$ mm/s and was neglected in comparison to the significantly larger scale of turbulent fluctuations in the flow.

Diagnostic techniques included determination of mean velocity profiles and turbulent fluctuations in the velocity by means of hot-wire anemometry using an AA Labs AN1005 anemometer. The hot-wire probe holder was affixed to a Velmex (VXM Model 1) stepping motor, which allowed positioning of the probe to within 2.5 microns. The probe position was initially measured by imaging from a Nikon (DS300) digital camera positioned adjacent to the test section; thereafter the motor incremented the position of the probe holder away from the plate, under the control of a LabView automation routine. The sampling frequency was $f_s = 60$ kHz, with record lengths of $2 - 6 \times 10^6$ samples.

Oil film interferometry was used to investigate the skin friction distribution downstream of the roughness associated with relaxation of the boundary layer. The interferometry was performed with 50 cSt silicone fluid (CAS 63148-62-9) deposited on the surface of the acrylic flat plate. The approximately 1 cm diameter oil droplet was illuminated by a 50 W sodium lamp and its spreading was recorded over time with the Nikon camera using a $1:1$ macro lens. The interference pattern was then processed by FFT to obtain the rate of oil thinning and thereby the wall shear stress. While this technique is strictly suitable only for steady flows, it is anticipated that the error due to the periodicity of the roughness amplitude in the dynamic case decays rapidly away from the roughness impulse and therefore this is a relatively accurate means to determine the local skin friction (although this assumption is under current study). Alternatively, the local skin friction can be approximated by indirect methods such as the Clauser plot or Preston probes only with the understanding that the lack of boundary layer equilibrium violates basic assumptions concerning the form of the mean velocity profile; a comparison is made between the two methods, the latter of which was used in the classical experiments.[17]

III. Results

Smooth wall measurements were taken with the hot-wire probe along the length of the tunnel before exchanging the smooth plate for the roughness apparatus. Measurements for smooth, static, and dynamic roughness cases were performed at three streamwise positions downstream of the roughness. The key parameters used for normalizations are shown in Table 1.

Measurement Location [m]		Smooth	Static	Dynamic	$u_\tau[m/s]$	
LE (x_l)	Roughness (x_r)	δ_{99} [m]	$\delta_{99}^{(s)}$ [m]	$\delta_{99}^{(d)}$ [m]	Oilfilm	Clauser
0.935	0.055	0.0166	0.0166	0.0172	1.01	0.85
1.250	0.270	0.0218	0.0223	0.0222	0.96	0.79
1.520	0.540	0.0249	0.0249	0.0259	0.95	0.80

Table 1. Experimental parameters at measurement locations. x_l and x_r are the distances from the leading edge and the start of the roughness impulse, respectively.

The oil film measurements tended to produce a value for u_τ around 10% higher than that inferred from the slope of the velocity profile in the log-law region (where $\kappa = 0.41$). The lower values tended to provide a better collapse with previously published profiles so those values were used for scaling turbulent fluctuations and spectra pending a more careful analysis of the oil film results. Each profile was scaled by its appropriate value of δ_{99}, but the streamwise distance was measurement in terms of the smooth wall value corresponding to the flow just downstream of the roughness ($\delta_{99} = 0.0166$).

The mean velocity profiles for the smooth wall, static roughness and dynamic roughness are shown in figure 3. Note that these plots are normalized using the freestream velocity and the local boundary layer thickness for each roughness case. As expected from simple r.m.s. arguments, the static roughness has a stronger effect on the shape of the mean velocity profiles than the dynamic roughness, but in each case the flow has almost returned to the undisturbed (smooth) profile by a distance of 40 boundary layer thicknesses downstream of the roughness.

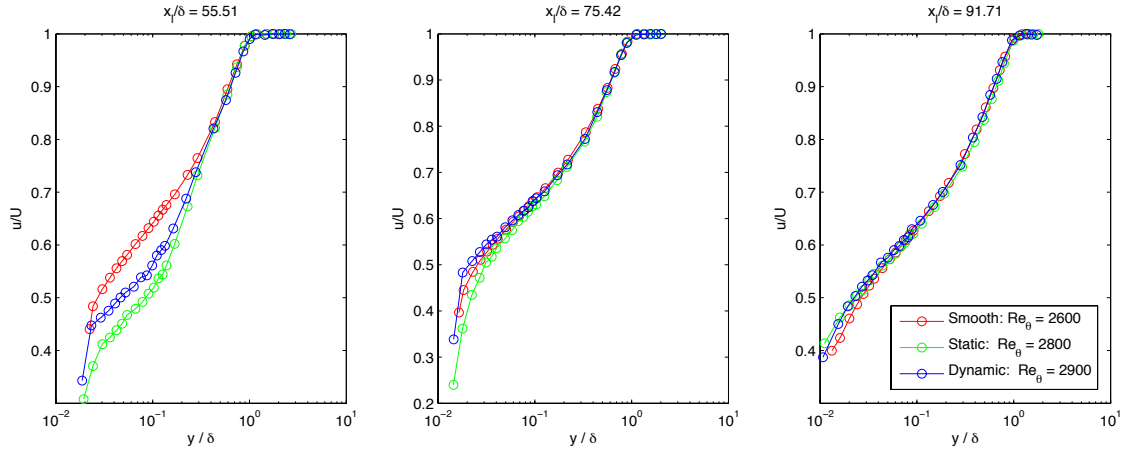

Figure 3. Development of the mean velocity profiles for nominal 20 m/s freestream with $k/\delta = 0.054$ and dynamic roughness at $f\delta/U_\infty = 0.0249$. The streamwise position x_l is measured from the leading edge of the plate.

The development of the turbulent fluctuations (figure 4) similarly indicates an approximate return to smooth wall behavior at the most downstream measurement location. Close to the dynamic roughness, there is additional streamwise energy close to the wall as compared to the static roughness case, indicating a significant difference in the response of the flow to the time-varying perturbation. In order to examine further impact of the static and dynamic roughness, time series were collected for spectral analysis at the wall normal positions where the turbulence signal indicated the greatest contrast between the flow regimes.

The spectral analysis shown in figure 5 reveals that both static and dynamic roughness perturbations alter both the spatial and spectral distributions of turbulent energy across the boundary layer, generally increasing the level above the smooth wall case, as would be expected for this deviation from equilibrium. Interestingly, for the dynamically rough case the 30 Hz oscillation contributed by the dynamic roughness persists throughout the boundary layer and beyond, as far as $1.7y/\delta$, but by $y/\delta = 2.8$ no trace of the perturbation signal remains. The intensity of the signal appears to strengthen moving away from the plate, achieving a maximum somewhere between $y^+ = 20$ to 160,

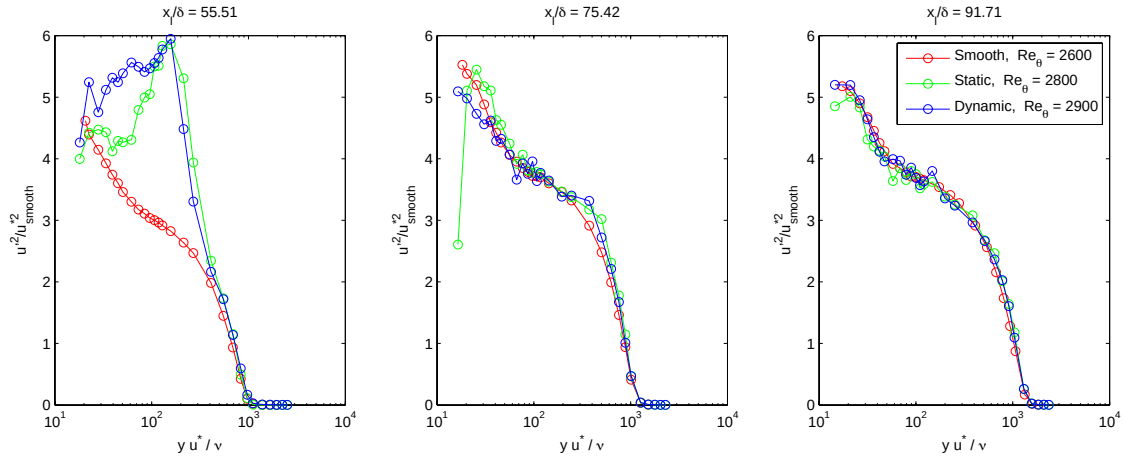

Figure 4. Development of the streamwise turbulence intensity, $\overline{u'^{2+}}$. Inner units are defined using the value of $u_\tau = 0.85$ from the smooth wall case.

suggesting that the effect of the dynamic roughness, which in a linear sense can be considered as the superposition of identical upstream- and downstream-propagating waves, is to force a perturbation in the fluid that is coherent up to the instantaneous edge of the boundary layer However, the generation of harmonics of the forcing frequency, clearly visible in figure 5, indicate that the actuation cannot be treated as a linear disturbance.

In order to track the development of internal layers within the boundary layer, as a consequence of the roughness, successive velocity profiles were recorded in close proximity to one another in order to allow for streamwise spatial differentiation of the profiles. The internal layers are identified by locating relative minima in the quantity $\left|\frac{du}{dx}\frac{\delta}{U_\infty}\right|$ where the spatial derivative is calculated by numerical difference between adjacent velocity profiles (figure 6). The results of this process are extraordinarily noisy, although with careful plotting, some relative minima can be isolated with reasonable confidence. Many of the extrema remain ambiguous and thus a more robust method for identifying internal layers is needed.The minima are then plotted by streamwise and wall-normal location in order to assemble the shape of the development of the internal layers in figure 7.

The dynamic roughness appears to develop a thinner internal layer than the static roughness of the same height, although no minima corresponding to the δ_1 layer could be located with any confidence for the dynamic case.

Figure 8 shows the variation of skin friction up- and down-stream of the roughness element obtained by oil film interferometry for both static and dynamic roughness elements. Prandtl's smooth wall curve is shown for comparison and the error bars represent the repeatability of the current oil film measurements. It is clear that for both roughness types, there is a skin friction reduction of order 10% immediately downstream of the perturbation, and that this is smaller for the dynamic roughness (as would be expected from consideration of the root-mean-square of roughness height). In addition, the skin friction appears to overshoot the smooth wall curve. Further mean velocity profiles will investigate the relaxation of the boundary layer in both cases. The estimates of skin friction obtained by using a Clauser fit to the velocity profiles are also shown in figure 8 as lone symbols. Clearly very large errors are inferred by assuming an equilibrium form for the mean velocity.

IV. Conclusion

We have presented first measurements of the return of a zero pressure gradient turbulent boundary layer towards equilibrium after perturbation by a spatial impulse of two-dimensional, dynamic roughness with a time-dependent amplitude. The response of the flow, in both mean and fluctuation streamwise velocities, has been shown to differ significantly from perturbation by a static roughness with the same peak amplitude. Determination of the variation of skin friction in this non-equilibrium flow remains challenging, but it is clear that very large errors are induced by the classical indirect methods.

The support of the Air Force Office of Scientific Research Boundary Layer Physics program under award #FA9550-08-1-0049 (program manager: John Schmisseur) is gratefully acknowledged.

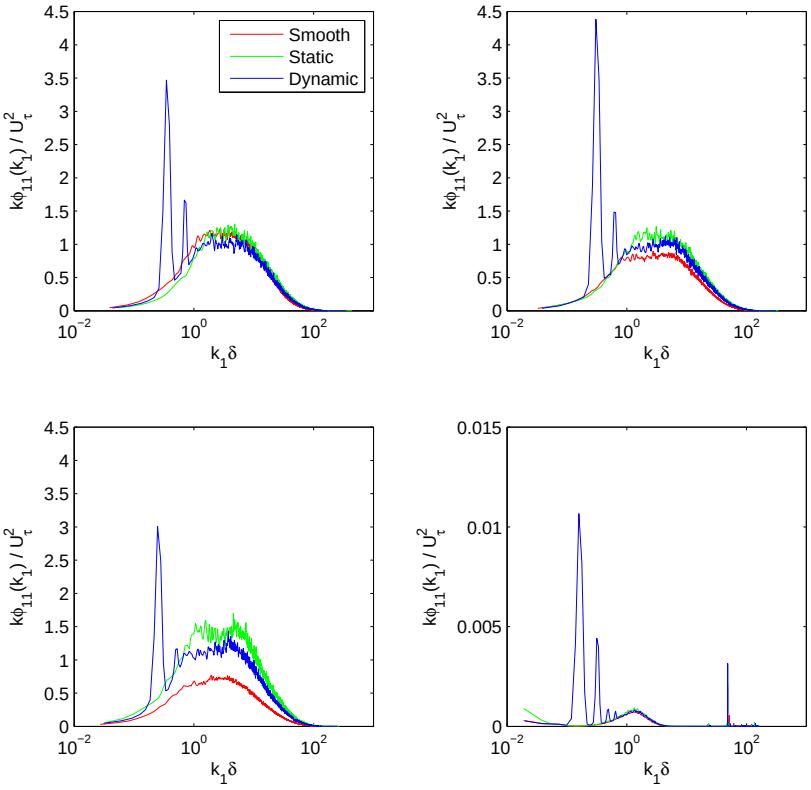

Figure 5. Development of the streamwise velocity spectra. Left to right, top to bottom: $y^+ = 22, 51, 157, 1686$. Inner units are defined using the value of $u_\tau = 0.85$ from the smooth wall case. The spectra are calculated from 2×10^6 points sampled at 60 kHz.

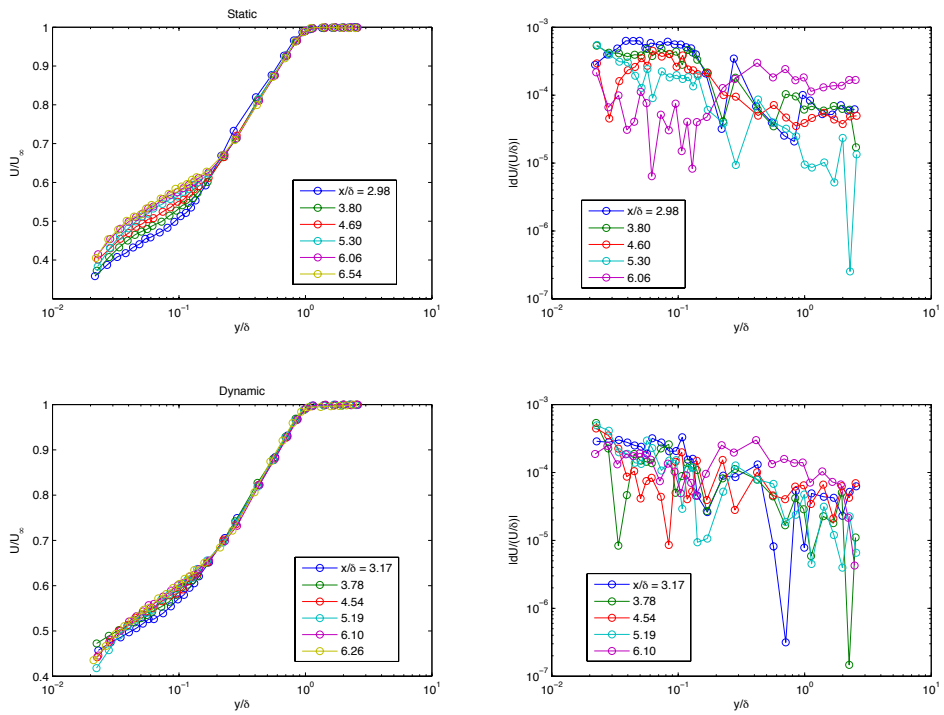

Figure 6. Successive mean velocities profiles in the streamwise direction, starting from the furthest upstream profile recorded previously, at $x/\delta = 55.5$ measured from the leading edge; for consistency with other results, the origin for the streamwise position x_r refers to the beginning of the roughness 880 mm from the leading edge, or about $x/\delta = 53.1$

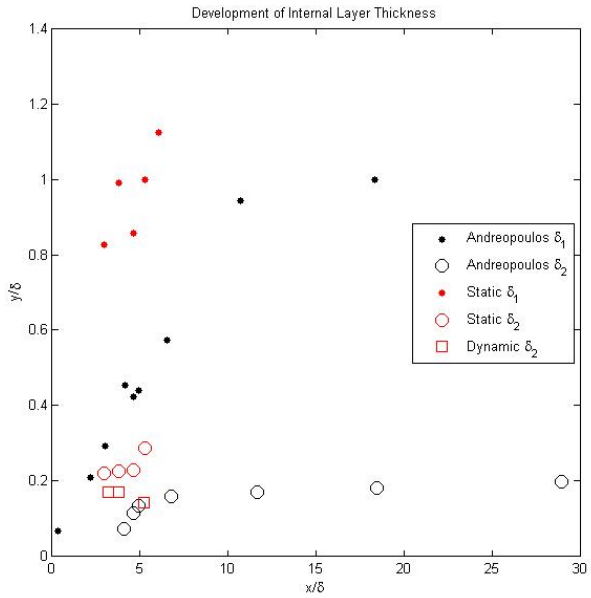

Figure 7. The minima of the consecutive velocity profile differences highlight internal layers within the boundary layer. The origin for the streamwise distance is the origin of the roughness. Data from Andreopolos and Wood[17] are included for comparison.

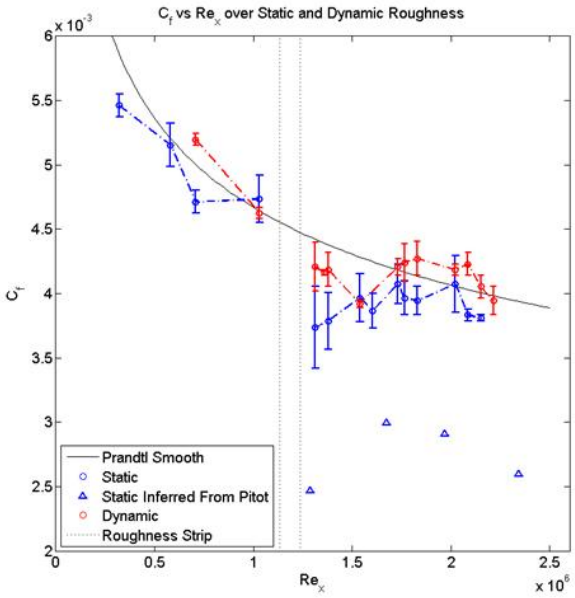

Figure 8. The variation of skin friction coefficient with downstream distance (non-dimensionalized with free-stream properties) for the smooth wall, static and dynamic roughness cases as obtained using oil film interferometry. The isolated symbols represent the estimates obtained using a Preston probe estimate for the static roughness case.

References

[1]Jiménez, J., "Turbulent flows over rough walls," *Annu. Rev. Fluid Mech.*, Vol. 36, 2004, pp. 173–196.

[2]Flack, K. A., Schultz, M. P., and Shapiro, T., "Experimental support for Townsend's Reynolds number similarity hypothesis on rough walls," *Phys. Fluids*, Vol. 17, No. 035102, 2005.

[3]Gioia, G. and Chakraborty, P., "Turbulent friction in rough pipes and the energy spectrum of the phenomenological theory," *Phys. Rev. Lett.*, Vol. 96, No. 044 502, 2006.

[4]Allen, J. J., Shockling, M. A., Kunkel, G. J., and Smits, A. J., "Turbulent flow in smooth and rough pipes," *Phil. Trans. R. Soc. A*, Vol. 365, 2007, pp. 699–714.

[5]Carlson, A. and Lumley, J. L., "Flow over an Obstacle Emerging from the Wall of a Channel," *AIAA Journal*, Vol. 34, No. 5, May 1996, pp. 924–931.

[6]McKeon, B. J., Lambert, S., Sherwin, S. J., and Morrison, J. F., "Active dimples for flow control," *Proc. 10th European Turbulence Conference*, Advances in Turbulence, CIMNE, November 2004.

[7]Endo, T. and Kasagi, N., "Active control of wall turbulence with wall deformation," *JSME Int. J., Series B*, Vol. 44, No. 2, 2001, pp. 195–203.

[8]Kim, C., Jeon, W.-P., Park, J., and Choi, H., "Effect of a localized time-periodic wall motion on a turbulent boundary layer flow," *Phys. Fluids*, Vol. 15, No. 1, 2003, pp. 265–268.

[9]White, E. B. and Saric, W. S., "Application of variable leading-edge roughness for transition control on swept wings," *AIAA 2000-0283*, 2000.

[10]Honsaker, R. and Huebsch, W., "Parametric study of dynamic roughness as a mechanism for flow control," *AIAA 2005-4732*, 2005.

[11]Orlandi, P., Leonardi, S., Tuzi, R., and Antonia, R. A., "Direct numerical simulation of turbulent channel flow with wall velocity disturbances," *Phys. Fluids*, Vol. 15, No. 12, 2003, pp. 3587–3601.

[12]Flores, O. and Jiménez, J., "Effect of wall-boundary disturbances on turbulent channel flows," *J. Fluid Mech.*, Vol. 566, 2006, pp. 357–376.

[13]Jiménez, J., Uhlmann, M., Pinelli, A., and Kawahura, G., "Turbulent shear flow over active and passive porous surfaces," *J. Fluid Mech.*, Vol. 442, 2001, pp. 89–117.

[14]Antonia, R. A. and Luxton, R. E., "The response of a turbulent boundary layer to a step change in surface roughness. Part 1. Smooth to rough." *J. Fluid Mech.*, Vol. 48, No. 4, 1971, pp. 721–761.

[15]Antonia, R. A. and Luxton, R. E., "The response of a turbulent boundary layer to a step change in surface roughness. Part 2. Rough-to-smooth." *J. Fluid Mech.*, Vol. 53, No. 4, 1972, pp. 737–757.

[16]Smits, A. J. and Wood, D. H., "The response of turbulent boundary layers to sudden perturbations." *Annu. Rev. Fluid Mech.*, Vol. 17, 1985, pp. 321–358.

[17]Andreopoulos, J. and Wood, D. H., "The response of a turbulent boundary layer to a short length of surface roughness." *J. Fluid Mech.*, Vol. 118, 1982, pp. 143–164.

[18]Perry, A. E., Schofield, W. H., and Joubert, P. N., "Rough wall turbulent boundary layers," *J. Fluid Mech.*, Vol. 22, 1969, pp. 285–304.